Biomimetic N-Terminal Alkylation of Peptoid Analogues of Surfactant Protein C

Nathan J. Brown,[†] Michelle T. Dohm,[‡§] Jorge Bernardino de la Serna,[¶*] and Annelise E. Barron[†‡§*]
[†]Department of Chemical and Biological Engineering, Northwestern University, Evanston, Illinois; [‡]Department of Bioengineering and [§]Department of Chemical Engineering, Stanford University, Stanford, California; and [¶]Department of Physics and Chemistry, MEMPHYS-Center for Biomembrane Physics, University of Southern Denmark, Odense, Denmark

ABSTRACT Surfactant protein C (SP-C) is a hydrophobic lipopeptide that is critical for lung function, in part because it physically catalyzes the formation of surface-associated surfactant reservoirs. Many of SP-C's key biophysical properties derive from its highly stable and hydrophobic α-helix. However, SP-C's posttranslational modification with N-terminal palmitoyl chains also seems to be quite important. We created a new (to our knowledge) class of variants of a synthetic, biomimetic family of peptide mimics (peptoids) that allow us to study the functional effects of biomimetic N-terminal alkylation in vitro. Mimics were designed to emulate the amphipathic patterning, helicity, and hydrophobicity of SP-C, and to include no, one, or two vicinal amide-linked, N-terminal octadecyl chains (providing a reach equivalent to that of natural palmitoyl chains). Pulsating bubble surfactometry and Langmuir-Wilhelmy surface balance studies showed that alkylation improved biomimetic surface activities, yielding lower film compressibility and lower maximum dynamic surface tensions. Atomic force microscopy studies indicated that alkyl chains bind to and retain segregated interfacial surfactant phases at low surface tensions by inducing 3D structural transitions in the monolayer's fluid-like phase, forming surfactant-associated reservoirs. Peptoid-based SP-C mimics are easily produced and purified, and offer much higher chemical and secondary structure stability than polypeptide-based mimics. In surfactant replacements intended for medical use, synthetic SP mimics reduce the odds of pathogen contamination, which may facilitate the wider use of surfactant treatment of respiratory disorders and diseases.

INTRODUCTION

Lung surfactant (LS) is a complex lipid/protein material that reduces and controls alveolar surface tension (γ, mN/m) during respiration. This reduces the work of breathing and maintains alveolar patency, enabling normal respiration. Phospholipids (PLs) make up 80% of LS's biomass, and neutral lipids and surfactant proteins (SPs) each account for 10% (1). No single component is fully responsible for LS's emergent biophysical properties; rather, each species contributes to surface activity. Saturated PLs are responsible for LS's γ-reduction properties; however, these species are poor single-component LSs that adsorb slowly to the air/liquid (a/l) interface and fail to respread upon inhalation. The addition of unsaturated PLs and neutral lipids improves these properties to some extent. Although the hydrophobic SPs, SP-B and SP-C, are minor components of LS (2% (wt)), they improve surfactant adsorption and recycling of the lipid film during respiration, and are required for surface activity (2,3). SP-B and SP-C are critical constituents of animal-derived, exogenous surfactant preparations used for the treatment of infant respiratory distress syndrome, which occurs in premature infants who lack functional LS.

SP-C is the smaller of the two hydrophobic SPs, at just 35 residues (Table 1). The mature lipopeptide contains a high number of Val, Leu, and Ile, as well as an N-terminal palmitoylation motif, making SP-C exceedingly hydrophobic. SP-C's secondary structure is simple and dominated by a large, 37-Å-long helical region (residues 9–34) (4). In an interfacial lipid system, SP-C reorients to maximize interactions between its poly-Val helix and the film's lipid acyl chains (5). SP-C's strong lipid association is further enhanced by two cationic residues as well as two palmitoylated cysteine residues (positions 5 and 6) that promote electrostatic and hydrophobic associations, respectively, with anionic PLs (6).

Although it is a minor LS constituent, SP-C exerts dramatic effects on surface activity (7). SP-C in PL suspensions accelerates PL adsorption and transfer from the subphase to the air-liquid (a/l) interface, rapidly forming a surfactant layer (8). SP-C promotes binding of dispersed lipid vesicles to newly formed surfactant layers, and upon compression to high surface pressures (Π, mN/m), catalyzes the formation of stacked multilayers of excluded surfactant material (9–11). SP-C's interaction with these surfactant structures retains fluid-phase PLs at the interface, improving surfactant respreading and lowering the maximum γ (γ_{max}) during respiration.

Although SP-C's distinct molecular features facilitate PL interactions and promote biophysical functioning, they complicate its handling and that of synthetic peptide-based analogs (12). SP-C's high β-branched amino acid content creates a marginally stable helix when isolated from natural milieu, and yields a high propensity for inactivation via β-strand aggregation and amyloid-like fibril formation (13). Therefore, it is difficult to isolate native SP-C and

Submitted August 17, 2010, and accepted for publication April 18, 2011.
*Correspondence: aebarron@stanford.edu or joberse@memphys.sdu.dk
Editor: Ka Yee C. Lee.

0006-3495/11/09/1076/10 $2.00
doi: 10.1016/j.bpj.2011.04.055

TABLE 1 SP-C and peptoid sequences

Compound	Structure
Porcine SP-C	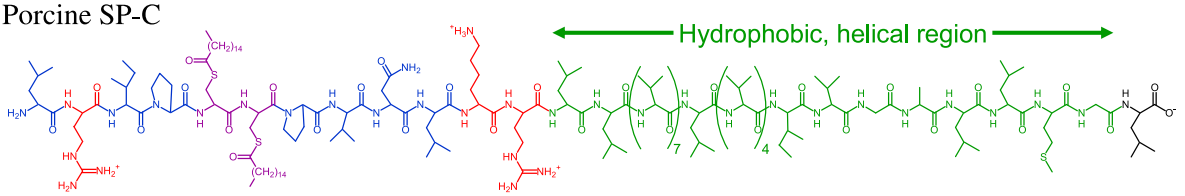
Peptoid 1	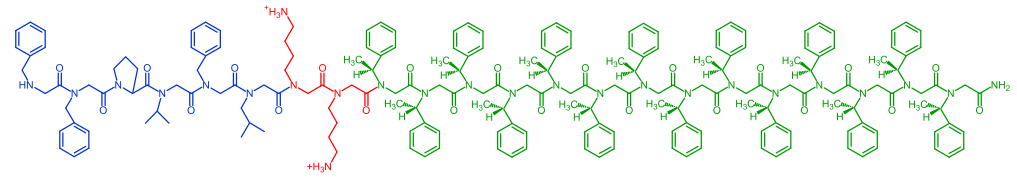
Peptoid 2	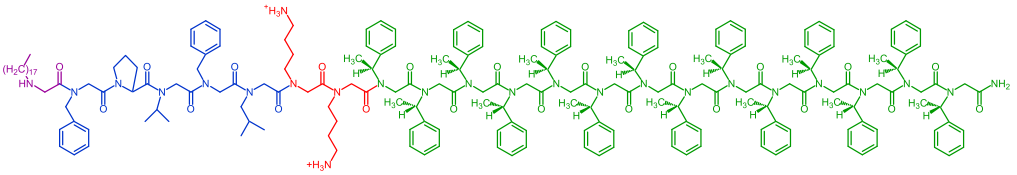
Peptoid 3	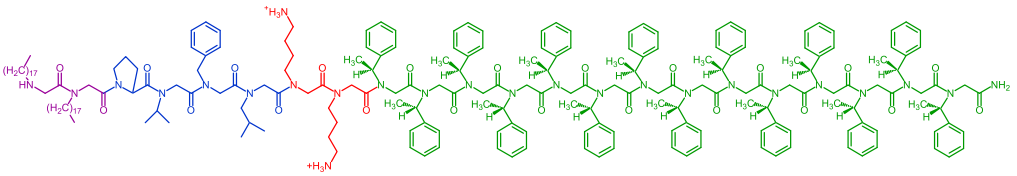

perform analog synthesis for the purpose of emulating or probing SP-C's mechanism (12).

A biomimetic approach that overcomes the difficulties associated with SP-C and peptide variants is to use poly-*N*-substituted glycines, or peptoids, as SP-C mimics (14,15). Peptoids share a common backbone structure with peptides; however, their side chains are displaced to the amide nitrogens (16). This renders peptoids invulnerable to proteases, thus enhancing their bioavailability. When substituted with chiral, bulky side chains, peptoids can adopt stable, polyproline-like helices that are stabilized by steric and, in some instances, electronic repulsions between aromatic side chains and carbonyl groups (17,18). Because peptoid helices are conformationally stable but lack backbone hydrogen bonding, they are ultrastable and do not aggregate over time (19). Peptoids are relatively easy and cost-effective to synthesize, with coupling efficiencies comparable to those of peptide synthesis. Therefore, peptoids are promising candidates for protein mimicry that requires helicity for function (14).

Here we expand on peptoid-based mimicry of SP-C by focusing on the N-terminal region. Although the hydrophobic helix contributes to many of SP-C's biophysical properties, evidence suggests that the N-terminal segment is responsible for important surface-active properties (6,20). To investigate the functional roles of palmitoyl-like modifications in peptoids, we created a series of nonalkylated and alkylated peptoids and characterized their in vitro surface properties in a synthetic PL formulation. Pulsating bubble surfactometry (PBS) and Langmuir-Wilhelmy surface balance (LWSB) measurements show that alkylation improves surface activity, resulting in reduced film compressibility and improved dynamic respreading as indicated by lower γ_{max}. Atomic force microscopy (AFM) results suggest that the alkyl chains retain interfacial surfactant material at low γ by inducing two- to three-dimensional (2-3D) structural transitions in the monolayer's fluid-like phase. Therefore, SP-C-like N-terminal alkyl chains are able to assist the formation of surfactant reservoirs that facilitate respreading and reduce γ_{max} during dynamic cycling, consistent with behavior observed for native SP-C.

MATERIALS AND METHODS

Materials

Peptoid synthesis reagents, primary amines, and palmitic acid (PA) were obtained from Sigma-Aldrich (Milwaukee, WI). Fmoc-protected proline

and Rink amide resin were obtained from NovaBiochem (San Diego, CA). The organic solvents used were high-performance liquid chromatography (HPLC) grade or better (Fisher Scientific, Pittsburgh, PA). DPPC and POPG were obtained from Avanti Polar Lipids (Alabaster, AL). Texas-Red 1,2-dihexadecanoyl-*sn*-glycero-3-phosphoethanolamine, triethylammonium salt (TR-DHPE) was acquired from Molecular Probes (Eugene, OR). The SP-C (a gift from Jesús Pérez-Gil) was extracted from porcine LS (21).

Peptoid synthesis

Peptoid-based SP-C mimics (Table 1) were synthesized (433A ABI synthesizer; Applied Biosystems, Foster City, CA) on solid phase according to the submonomer method (16). Crude products were purified by reversed-phase (RP)-HPLC (Waters) with a C4 column (Vydac) on a linear gradient of 40–90% solvent B in solvent A over 80 min (solvent A = 0.1% TFA in water, and solvent B = 0.1% TFA in isopropanol). Peptoid purities were confirmed at >97% by analytical RP-HPLC, and molar masses were confirmed by electrospray ionization mass spectrometry.

Pulsating bubble surfactometry

Static and dynamic characterization of film properties was performed on a modified pulsating bubble surfactometer (General Transco, Largo, FL) as previously described (22). The synthetic lipids (DPPC/POPG/PA, 68:22:9, by weight) were dissolved in chloroform/methanol (3:1 (v:v)) alone or with 2 mol % SP-C additive. Samples were dried and resuspended in aqueous buffer (150 mM NaCl, 5 mM $CaCl_2$, and 10 mM HEPES, pH 6.9) to a lipid concentration of 1 mg/mL. Samples were loaded onto the surfactometer at 37°C, a bubble (radius = 0.4 mm) was formed, and an image acquisition system used to determine bubble size and trans-film pressure. For static adsorption, γ versus time was recorded for 20 min. We then collected dynamic measurements of γ versus bubble surface area by cycling the bubble radius (0.4–0.55 mm, oscillation frequency of 20 cycles/min, 10 min). Static and dynamic PBS experiments were repeated a minimum of six times for each preparation. During dynamic cycling, the image analysis system sometimes failed to fit the bubble at low-γ due to shape deformation, causing an apparent break in the PBS loop. However, the pressure drop across the bubble was low in these instances, and the amount of deformation observed was significant, confirming that γ was <1 mN/m during breaks in the compression-expansion loops (22).

Langmuir-Wilhelmy surface balance studies and fluorescence microscopy

We obtained surface pressure (Π)-molecular area (A) isotherms using an LWSB (trough area 240 cm^2) as described previously (15). For each experiment, a buffered subphase (150 mM NaCl, 5 mM $CaCl_2$, and 10 mM HEPES at pH 6.9) was heated to 25°C or 37°C, and a Wilhelmy surface balance (Reigler & Kirstein, Berlin, Germany) was calibrated to monitor Π versus A. The surfactant sample in organic solution was spread at the interface via a syringe, and after solvent evaporation was completed (10 min), two Teflon barriers were compressed (22 $Å^2$/molecule/min). Each film underwent three compression-expansion cycles to onset of collapse and then expansion to high A. All LWSB experiments were reproducibly repeated at least six times.

A compact microscope stand (MM40; Nikon, Tokyo, Japan) with a 100 W mercury lamp was used to obtain fluorescence microscopy (FM) images on LWSB films. Fluorescence was detected by a Dage-MTI three-chip color camera (Dage-MTI, Michigan City, IN) in conjunction with a generation II intensifier (Fryer, Huntley, IL). Samples were spiked with 0.5 mol % of a fluorescently labeled lipid (TR-DHPE) for detection. Inclusion of the labeled lipid at this concentration did not alter the film morphology (23). FM experiments were performed on the same aqueous buffer subphase at 37°C with a barrier speed of 5 mm/min. Lipid domain coverage and sizes were calculated with the use of ImageJ (24).

AFM

We performed AFM imaging of interfacial monolayers using Langmuir-Blodgett (LB) technology, which involves the transfer of interfacial material to a solid support (25). We prepared supported surfactant monolayers by initially spreading surfactant material onto buffered subphase (5 mM Tris and 150 mM NaCl, pH 7.0) at 22°C in an LB trough (NIMA Technology, Coventry, UK) to a Π of ~1 mN/m. After 10 min, the film was compressed (50 cm^2/min) to the desired Π and held for 5 min (for isotherms, see Fig. S1 in the Supporting Material). A previously immersed, freshly cleaved muscovite mica substrate (Plano, Wetzlar, Germany) was then lifted at constant speed (10 mm/min) to deposit the surface layer onto the mica substrate. The deposited LB films were dried overnight, and topographical images were taken at three locations per Π using an atomic force microscope (JPK NanoWizard, JPK Instruments, Berlin, Germany) in air tapping mode with silicon-SPM cantilevers (nanosensors; NanoWorld AG, Neuchâtel, Switzerland).

Statistical analysis

A one-way analysis of variance with post hoc Tukey-Kramer multiple comparison testing was used for analysis of results ($p < 0.05$).

RESULTS

Peptoid design and rationale

Efforts to develop a functional peptoid-based SP-C mimic have incorporated SP-C's important molecular and structural features, including its extreme hydrophobicity, overall positioning of polar residues, and rigid helix (14). Detailed structure-function studies with these mimics focused on optimizing the helix length and side-chain chemistry (15), and revealed that a helix length of 28 Å, in similarity to SP-C's Val-rich region, gave rise to favorable surface activity. In addition, it was discovered that preserving the rigid nature of the helix was best accomplished with the use of bulky aromatic rather than aliphatic side chains, despite the aliphatic nature of SP-C's helix.

Recent studies with peptide-based SP-C constructs showed that the N-terminal region, including the thioester-linked palmitoyl chains, plays an important biophysical role in SP-C-related surfactant homeostasis (20,26). To investigate the analogous role of alkyl chains in a peptoid, we incorporated octadecylamine (*N*ocd) at the N-terminus of our mimics. *N*ocd is a C18 primary alkyl amine that approximates the length and hydrophobicity of a palmitoyl chain, including the thioester bond. The alkyl chain was selectively introduced on-resin during synthesis (the amide linkage is stable against hydrolysis under alkaline conditions, eliminating the need for purification steps postalkylation and minimizing exposure to harsh reaction conditions). We created three analogs, termed peptoids 1, 2, and 3, which

had no, one, or two *N*ocd residues at the N-terminus, respectively (Table 1). These analogs mimic SP-C residues 5–32 by having 14 α-chiral, aromatic residues in the helix along with an achiral N-terminal stretch that grossly mimics the human SP-C sequence. The free-solution SP-C mimics were similarly helical by circular dichroism (CD) (Fig. S2), with aromatic peptoid helix spectra that resembled those of well-defined polyproline type I-like helices at 3 residues/turn and a 6 Å pitch (15). Independently of the alkyl chains, the designed mimics replicate SP-C's hydrophobicity, amphipathicity, and helicity.

PBS

An essential biophysical property of LS is its ability to rapidly adsorb from the alveolar subphase to the a/l interface, forming a surface-active layer that regulates γ during respiration. PLs exhibit poor adsorption kinetics; however, the inclusion of hydrophobic SPs yields surfactants that reach an equilibrium γ (γ_{eq}) of 25 mN/m in <1 min (8,27). The lipid mixture adsorption kinetics with and without the addition of 2 mol % SP-C or SP-C mimics were characterized on a modified PBS in static mode (Fig. S3). The peptoid-enhanced formulations improved the surfactant adsorption rate to γ_{eq}-values of 30–32 mN/m, though less than the natural porcine SP-C formulation. The presence of one or two alkyl chains in the peptoid at this concentration did not affect the already favorable surfactant adsorption behavior.

LS is remarkably able to minimize pressure inequalities and maintain patency among the alveoli, resulting in near-zero γ during respiratory expiration and rapid respreading on inspiration, the latter reducing γ_{max}. To assess the ability of peptoid-based formulations to reduce and control γ as a function of surface area at physiological rates, we performed dynamic PBS experiments at 37°C with an oscillation frequency of 20 cycles/min and 50% reduction in surface area. Important features for a biomimetic surfactant in compression-expansion loops include a low minimum γ (γ_{min}) with minimal compression (low compressibility), and a low γ_{max} indicating rapid respreading upon expansion (28). PBS parameters (Table 2) and representative PBS compression-expansion loops after 5 min of cycling are presented in Fig. 1 *A*. For the γ_{max} and % compression values shown in Table 2, all formulations were similar to each other but different from the lipid formulation alone.

The lipid mixture exhibited a high γ_{max} and γ_{min} of 64 mN/m and 12 mN/m, respectively (Fig. 1 *A* and Table 2). In addition, the film surface area compression to $\gamma < 20$ mN/m was 45%. Adding SP-C to the lipid mixture improved the surface activity of the film, as indicated by the lower γ_{max} of 36 mN/m and a γ_{min} of <1 mN/m. The presence of SP-C also decreased the compressibility of the surfactant, with 8% compression to reach $\gamma < 20$ mN/m. These features were similar to those of Infasurf, a clinical surfactant replacement therapy that contains both SP-B and SP-C (22).

The addition of peptoid to the lipids improved dynamic film behavior in a manner similar to that observed for SP-C (Fig. 1 *A* and Table 2). Addition of peptoid 1 to lipids reduced both γ_{max} and γ_{min} to 51 mN/m and <1 mN/m, respectively. Inclusion of peptoid 1 also reduced the amount of compression necessary to reach a $\gamma < 20$ mN/m to 30%. The improvements in dynamic surface activity observed with the peptoid 1 formulation are similar to those observed with a nonacylated, synthetic, and peptide-based SP-C mimic (15).

Compression-expansion loops for films containing alkylated mimics showed greater improvement in dynamic surface-active properties relative to those for peptoid 1. Adding one or two alkyl chains to the peptoid similarly reduced γ_{min} to <1 mN/m, but the γ_{max}-values for the peptoid 2 and 3 formulations were reduced to 45 mN/m (versus 51 mN/m), indicating faster respreading upon film expansion (Fig. 1 *A* and Table 2). The amount of compression to reach 20 mN/m also decreased to 25% and 23% for peptoids 2 and 3, respectively. The addition of at least one alkyl chain appeared to cause a favorable interaction with the lipids, engendering a reduction in surface film compressibility as well as an improved interfacial surfactant material retainment and replenishment upon expansion.

LWSB studies

To characterize the influence of the peptoids on monolayer phase behavior and lipid respreading, we obtained LWSB

TABLE 2 Dynamic PBS results

Formulation	1 min		5 min		10 min		
	γ_{max}	γ_{min}*	γ_{max}	γ_{min}*	γ_{max}	γ_{min}*	% Compression†
Lipids	65.4 ± 3.4	12.9 ± 4.0	64.2 ± 2.8	12.2 ± 1.8	63.0 ± 4.0	12.1 ± 2.1	45.1 ± 4.0
Lipids + SP-C	37.0 ± 2.4	< 1	36.3 ± 2.2	< 1	35.4 ± 2.0	< 1	8.0 ± 2.4
Lipids + peptoid 1	50.8 ± 2.2	< 1	51.1 ± 1.3	< 1	51.0 ± 1.6	< 1	30.5 ± 2.2
Lipids + peptoid 2	46.1 ± 3.5	< 1	45.1 ± 2.8	< 1	44.4 ± 2.4	< 1	25.1 ± 3.2
Lipids + peptoid 3	46.3 ± 3.2	< 1	45.5 ± 2.2	< 1	44.8 ± 3.2	< 1	22.9 ± 2.5

Data are mean γ ± SD in mN/m. For γ_{max} and % compression, all groups were significantly different ($p < 0.05$) from each other except for Lipids + Mimic pC and Lipids + Mimic di-pC at each time interval. For γ_{min}, all SP-C and SP-C mimic formulations were similar to each other and different from Lipids.
*All experimental runs reached a $\gamma_{min} < 1$ mN/m except for formulations comprised of lipids without any added SP-C analog.
†Compression refers to the percent relative compression necessary to reach a $\gamma < 20$ mN/m.

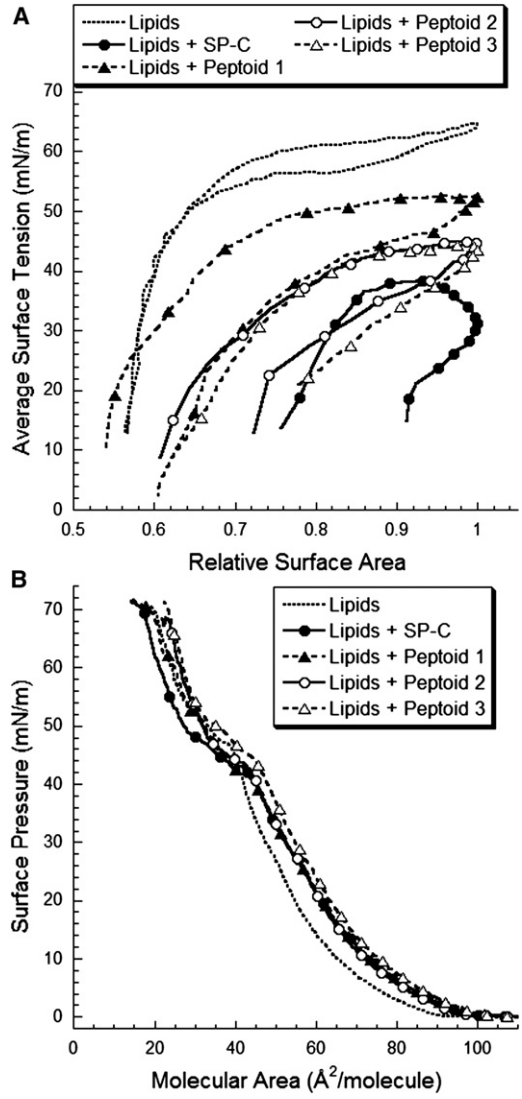

FIGURE 1 Dynamic PBS results as γ versus relative surface area (surface area/maximum surface area) at 20 cycles/min for 5 min. (*A*) The bulk surfactant concentration was 1 mg/mL lipids (DPPC/POPG/PA, 68:22:9 (wt)) at 37°C. First compression surface pressure (Π)-area (*A*) LWSB isotherms for the formulations were collected on a buffered subphase at 37°C. (*B*) LWSB molecular areas include all surfactant species, lipid plus SP-C/peptoid.

Π-A isotherms at both 25°C and 37°C for three successive compression-expansion cycles. Representative first compression isotherms are shown for lipids alone, with porcine SP-C, and with mimics at 37°C (Fig. 1 *B*). We determined the relative respreading by comparing the ratio of liftoff A's (defined as the A at which Π first increases) as well as at 30 mN/m between the first and third compressions (Table 3). Results obtained at 25°C were comparable (Fig. S4 and Table S2).

The lipid isotherm lifted off at an A of 98 Å^2/molecule (Fig. 1 *B*) with a shallow slope up to 10 mN/m. As the film was compressed from 10 to 44 mN/m, the isotherm's slope increased, indicating less film compressibility. Further lipid film compression led to a kink, or structural transition to a metastable state, at 47 mN/m (29). The film reached a high Π of 72 mN/m (near-zero γ), or collapse. The presence of SP-C in the lipids at the interface shifted the liftoff to a greater A of 102 Å^2/molecule, indicating increased surface activity and an earlier transition to an LE state. At lower Π, the isotherm resembled that of lipids alone, but shifted toward higher A. However, further compression resulted in a dramatic plateau region beginning at 43 mN/m, likely due to increased structural rearrangement in the surface layer. The SP-C-containing formulation also collapsed at 72 mN/m.

Inclusion of the nonalkylated peptoid 1 in the lipids increased the liftoff A to 104 Å^2/molecule, in similarity to SP-C (Fig. 1 *B* and Table 3). The isotherm was nearly identical to the formulation containing SP-C until, at 42 mN/m, a less pronounced biomimetic plateau region was observed. The peptoid 1 formulation also exhibited a high collapse Π of 72 mN/m. Introducing one alkyl chain to the peptoid's N-terminus resulted in an isotherm nearly identical to peptoid 1, with a liftoff A of 105 Å^2/molecule and a plateau region starting at 43 mN/m. A second peptoid alkyl chain increased the liftoff to 110 Å^2/molecule for peptoid 3. Compression of the peptoid 3 film revealed less compressibility than the other formulations, and a plateau region that was most similar to the SP-C formulation (Fig. 1 *B*).

To assess peptoid-enhanced surfactant respreading, we compared the isotherm A's at liftoff and 30 mN/m on the third compression with those of the first compression (Table 3). The third compression isotherms were similar to the first compression (Fig. S4 and Fig. S5), but each formulation shifted toward smaller A with successive compressions, indicating loss of surfactant material to the subphase. Relative to the lipids, the lipid-SP-C formulation improved the relative recovery of surfactant material at both the liftoff A and 30 mN/m (82% and 83% vs. 73% and 79%, respectively; Table 3). Addition of peptoid to the lipids also resulted in improved surfactant respreading at the liftoff A and at 30 mN/m. However, no significant differences ($p > 0.05$) were observed among the peptoid mimics.

FM film morphology imaging

We obtained greater insight into specific lipid-SP-C mimic interactions by performing FM of the surface film morphology with respect to Π. This technique enables direct visualization of certain aspects of the a/l interfacial surfactant monolayer, and the impact that added species have on the formation of surfactant domain structures. Film FM images at 37°C, with 0.5 mol % TR-DPHE added, are shown in Fig. 2, both below (panels *A–E*) and above (panels *F–J*) the plateau region. TR-DPHE is a fluorescently labeled PL that is excluded from the more-ordered, liquid condensed (LC) lipid phase upon close lipid packing during compression; therefore, dark regions in the FM images

TABLE 3 LWSB compression and percent recovery data

	First compression		Third compression		% Recovery*	
Formulation	Liftoff area	Area at 30 mN/m	Liftoff area	Area at 30 mN/m	Liftoff	30 mN/m
Lipids	98.3 ± 4.2	48.2 ± 1.7	72.1 ± 4.2	38.2 ± 2.5	73.5 ± 4.9	79.3 ± 6.0
Lipids + SP-C	102.3 ± 0.7	52.2 ± 0.8	84.3 ± 3.3	43.5 ± 3.2	82.4 ± 3.1	83.2 ± 5.1
Lipids + peptoid 1	104.0 ± 2.0	51.9 ± 0.6	80.8 ± 3.4	41.6 ± 3.0	77.8 ± 4.4	80.2 ± 6.0
Lipids + peptoid 2	105.3 ± 2.2	53.8 ± 1.4	82.6 ± 5.1	43.8 ± 2.7	78.9 ± 6.1	81.5 ± 5.4
Lipids + peptoid 3	109.6 ± 4.9	53.9 ± 1.3	85.9 ± 4.9	45.8 ± 2.4	78.3 ± 2.6	85.0 ± 4.9

Data are the mean ± SD in Å^2/molecule for areas and % for recoveries.
*Term "% Recovery" refers to the percent molecular area at either liftoff or 30 mN/m on the third compression relative to the molecular area of the corresponding feature on the first compression.

represent the ordered LC phase, and lighter regions correspond to the more fluid liquid expanded (LE) phase.

The pure lipid system displayed nucleation of dark LC domains at 25 mN/m that grew in size upon further compression (Fig. 2, *A* and *F*). At 35 mN/m, the lipid film exhibited dark LC domains that ranged from 30 to 170 μm^2 in area and occupied 18% of the analyzed film area. Addition of either SP-C or mimics to the lipids resulted in similar film morphologies at 35 mN/m (Fig. 2, *B–E*). The formulations all displayed coexisting LE and LC domains that were similar to those of the lipid-only film. The relative size of the LC domains was the main difference between the SP-C/mimic-containing formulations and the lipid film, where the LC domain sizes were reduced to 25–50 μm^2. In addition, the alkylated mimics reduced the LC domains to a greater extent than did peptoid 1. LC domain fractional area coverages were all 10–17% and not significantly different from the lipid film.

Increasing the lipid film Π to 50 mN/m resulted in LC domain coalescence and a larger average size (190 μm^2) that occupied the same 22% area observed at 35 mN/m (Fig. 2 *F*). The SP-C and peptoid-enhanced film morphologies were similar at 50 mN/m, but in contrast to the case at 35 mN/m, they differed from those of the lipid film. The SP-C formulation LC domains remained the same size (20 μm^2) as observed at 35 mN/m and covered the same 17% film area. SP-C also induced the formation of small, bright domains in the LE phase, known as 3D protrusions (30). These observations are consistent with previous SP-C experiments in which it partitioned into the fluid-like phase of the monolayer, altering the lipid packing and causing film perturbations (31,32) that are important SP-C-linked characteristics (26,33,34).

The morphology of the peptoid 1 formulation at 50 mN/m was similar to that observed at 35 mN/m, with LC domains of 50 μm^2 that occupied the same film area. Peptoid 1 also resulted in the occurrence of bright structures, but their abundance was less than that observed for the SP-C formulation. Peptoids 2 and 3 produced similar film morphologies, with an average LC domain size of 35 μm^2 and 47 μm^2, respectively, and 12% film coverage. The film's 3D protrusions were present in greater abundance and more similar to those of the SP-C film. Therefore, all peptoid-based mimics strongly interacted with lipids, indicating enhanced surface activity as Π increased.

AFM

SP-C modulates the fluid lipid phase in compressed lipid films by inducing 3D structural transitions, forming a

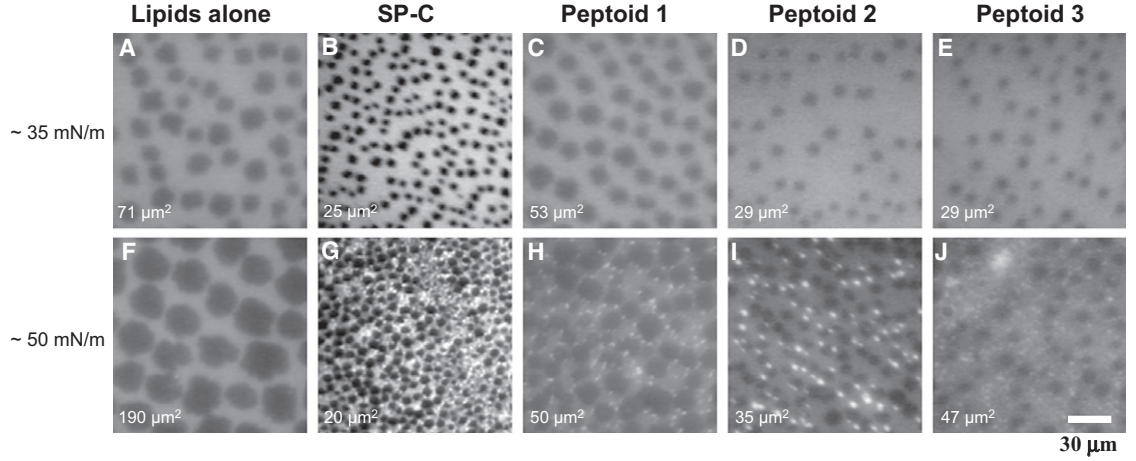

FIGURE 2 FM micrographs at 37°C corresponding to Π of 35 mN/m and 50 mN/m for DPPC/POPG/PA (68:22:9 (wt)) alone (*A* and *F*), with 2 mol % SP-C (*B* and *G*), peptoid 1 (*C* and *H*), peptoid 2 (*D* and *I*), and peptoid 3 (*E* and *J*). Average LC domain (*dark area*) is indicated at the lower left of each panel.

surfactant reservoir at higher Π (10,26,33). This effect is particularly enhanced in the presence of the palmitoyl chains. To investigate the influence of SP-C-like alkylation in the SP-C constructs in a lipid film, we used AFM to study the film morphology and topography of peptoid 1 and 3 films at two Π points. AFM provides the relative height of interfacial structures at various compression states, and offers direct mechanistic insight into the observed surface-activity differences between peptoids 1 and 3. Because peptoids 2 and 3 showed statistically similar behaviors, only peptoid 3 was characterized by AFM. This similarity is both expected and consistent with variations in SP-C palmitoylation across different species (i.e., canine SP-C contains only one palmitoyl chain).

Fig. 3 *A* shows the AFM images for the lipid film below and above the plateau region at 30 mN/m and 60 mN/m, respectively. Below the plateau region, we observed the coexistence of both LE and LC domains, consistent with the FM images (Fig. 2 *A*). At this Π, both large (25–35 μm) and small (4–6 μm) irregularly shaped LC domains were present in an interconnected fluid LE phase. We also observed phase boundary holes or defects in condensed regions, likely resulting from LE phase incorporation (10). Height differences between the LC and LE phases at 30 mN/m were 0.5–1.0 nm, consistent with expected height differences between gel and fluid lipid phases (10).

Compression of the lipids to 60 mN/m led to an interfacial film that was somewhat uniform in height (Fig. 3 *A*). LC domains increased in size and appeared to be pushed together, with some fluid-like phase remaining. This is seemingly in contrast to the FM images, where phase coexistence was observed up to the surface layer collapse; however, it is believed that the observed fluid LE-like phase is actually a metastable state with thickness comparable to that of the LC phase (35). At higher Π, a few protrusions 5–10 nm high were observed in the formerly fluid phase, consistent with multilayers of excluded material (10).

At 30 mN/m, addition of either peptoid 1 or 3 to the surfactant resulted in a film with large, multilobed LC domains similar to those observed for the lipids alone; however, much smaller and interspersed LC-like structures were also observed in the LE region (Fig. 3, *B* and *C*). Small and large LC domain heights were consistent and 1 nm greater than those of the fluid LE region. As the peptoid 1 and 3 films were compressed, the large LC domains increased in size, whereas the smaller structures fused together, forming an interconnected LC phase network among the LE region (data not shown). For peptoid 1, film compression caused the fusion of the LC framework, with only large LC domains and no fluid region (Fig. 3 *B*). The peptoid 1 formulation at 60 mN/m was similar to the lipid-only film, with no appreciable height difference between the regions and a few bright protrusions 5–7 nm higher than the surrounding film. Above the plateau region at 60 mN/m, the AFM surface topography was distinct for the peptoid 3 film relative to the lipid-only or peptoid 1 films (Fig. 3 *C*). In contrast

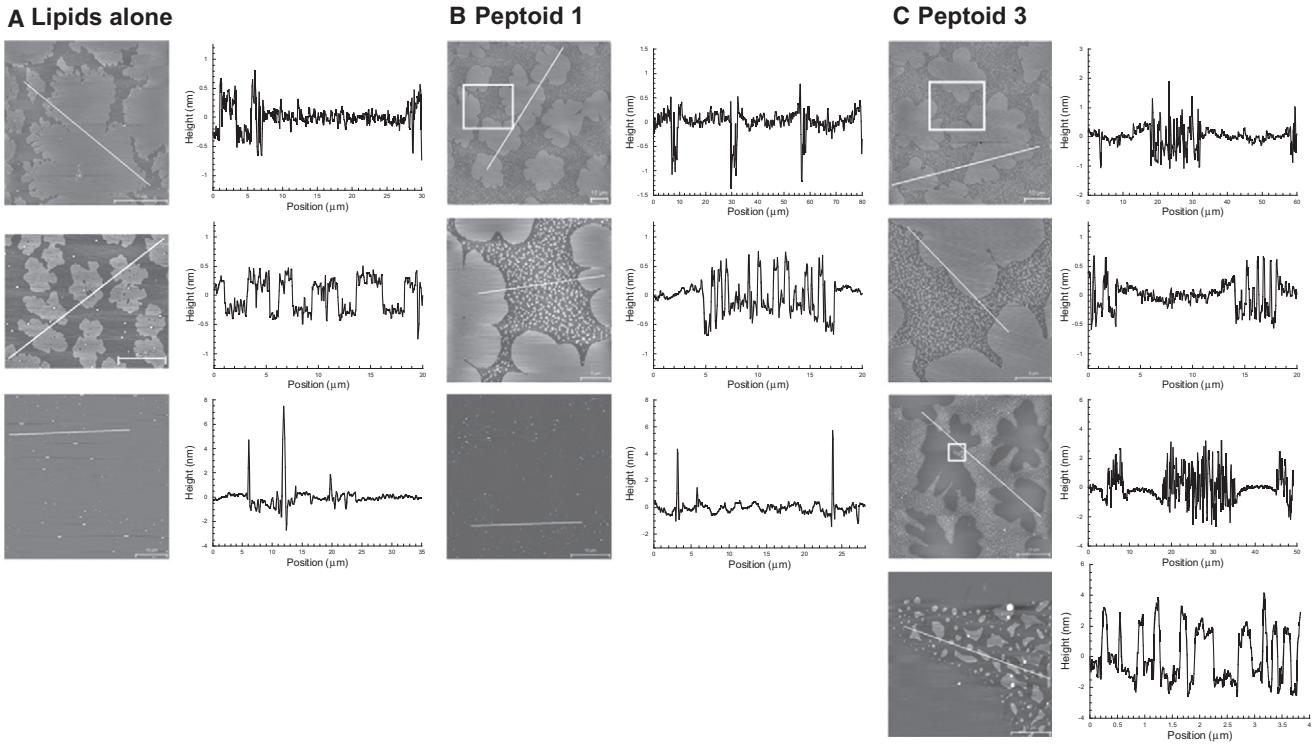

FIGURE 3 AFM images and height profiles for lipids alone (DPPC/POPG/PA, 68:22:9 (wt)) (*A*), plus 2 mol % of peptoid 1 (*B*) and peptoid 3 (*C*) at Π of 30 mN/m and 60 mN/m. A detailed AFM image of the square inset area is presented below the corresponding image.

to a film more uniformly composed of fused LC-appearing domains, the multilobed LC domains remained segregated within a second interfacial phase derived from the fluid phase. The former LE region was thicker, with large, 5-nm-high protrusions, suggesting multilayers of excluded material still associated with the a/l interface (10). This elevated and interconnected network of excluded surfactant material is consistent with previous studies of SP-C in highly compressed lipid films, in which SP-C facilitated reversible protrusions of stacked bilayers to form a surfactant reservoir attached to the film (10,26).

DISCUSSION

In this study, we mimicked SP-C palmitoylation in peptoids by incorporating *N*ocd at the achiral N-terminus, preserving both the hydrophobicity and length of the palmitoylated cysteine residues in SP-C. Although all of the mimics replicated many of the in vitro surface activities of native SP-C, the greatest biomimicry was obtained upon peptoid N-terminal alkylation.

Although alkylation increased the helicity of SP-C by stabilizing the helix, no alteration in peptoid helicity was observed for the mimics (5). Because peptoid helices are derived from steric repulsions, the helix is confined to the location of the chiral residues and does not change upon alkylation. Therefore, any changes in activity due to alkylation were independent of secondary structure. Similarly, despite the increase in hydrophobicity after alkylation, no change was observed in surfactant adsorption rates at the concentrations studied. It is likely that the peptoids are already sufficiently hydrophobic to promote rapid interfacial adsorption of the dispersed surfactant material. In addition, the alkyl chains are well incorporated into the dispersed surfactant and probably do not further perturb the interfacial lipid film or the suspended liposomes, and thus do not affect the two-step adsorption process (36).

Controlling γ as a function of surface area during the respiration cycle is a critical function of LS. An efficacious synthetic LS must reduce γ_{max} upon inspiration and attain near-zero γ_{min} upon exhalation immediately and continuously throughout the respiration cycle. Dynamic PBS loops revealed that the SP-C mimics reduced the γ_{max} and γ_{min} of the lipids, as well as the surfactant compressibility, in similarity to SP-C. Introducing either one or two alkyl chains to the peptoids markedly reduced the γ_{max} during dynamic cycling, representing a significant improvement in the film replenishment during surface expansion, which likely reduced the work of breathing in vivo (28). The alkyl chains also decreased the film compressibility to $\gamma < 20$ mN/m. These improvements led to PBS loops for the peptoid 2 and 3 films that were similar in shape to those for natural LS, albeit with higher γ_{max} (45 mN/m vs. 35 mN/m for natural LS). A possible explanation for the improved dynamic PBS characteristics postalkylation is that the alkyl chains act as hydrophobic lipid anchors, creating surface-associated surfactant reservoirs that both resist compression and are readily reincorporated upon film expansion, reducing both film compressibility and γ_{max} (35,37). Therefore, despite the dominant role of the helical region in many of the observed surface-active properties, the N-terminal palmitoyl-like chains also contribute to the surface activity of SP-C and SP-C-like species.

We evaluated the peptoids' ability to insert into and modulate a film, as well as influence surfactant respreading and monolayer phase behavior, using both quasi-equilibrium LWSB and FM. Isotherm improvements were, in general, modest and dominated by lipid behavior; however, favorable changes in structural organization and phase morphologies were observed at higher Π-values. Addition of either SP-C or peptoids to the film increased the liftoff area, largely due to the relative size of the added species at the a/l interface. No significant differences were observed for peptoids 2 and 3, indicating that the alkyl chains were well incorporated into the monolayer. Further film compression led to an isotherm structural transition in the presence of either SP-C or the peptoids, as observed by a kink or plateau at 42 mN/m. This kink is believed to coincide with a 2-3D structural transition in the film and the formation of surface-associated surfactant multilayer structures that reversibly unfold upon expansion (10,11,38). Plateau regions for the mimic-containing films were extended slightly postalkylation, indicating greater structural refinement; however, the effect was not as extensive as that observed for SP-C. The peptoids also improved the surfactant morphology similarly to SP-C, reducing ordered LC domain size at all Π-values. Above the plateau region, abundant protrusions were observed in the mimic-containing films that increased upon alkylation and were similar to SP-C, in agreement with the results of the LWSB spreading and PBS cycling experiments.

AFM was used to further probe for a mechanistic explanation of the observed differences in surface activities between peptoids 1 and 3, which differ only by alkylation. From the AFM images at low Π, we observed that both peptoids 1 and 3 altered the surfactant surface morphology. Both peptoid-containing formulations had large, multilobed LC domains surrounded by a more fluid LE phase, consistent with FM images. Numerous smaller domains within the LE phase were also present and protruded from the surrounding LE phase. However, as Π was increased, only the film containing peptoid 3 caused a thickening of the interconnected (formerly LE) region. This distinct phase was maintained along with the LC phase at high Π-values. These results are consistent with observations that natural SP-C and synthetic peptide-based analogs catalyze the formation of excluded surfactant structures that reversibly unfold upon expansion, as depicted previously (10,37,39).

The thickening of the fluid-like phase and maintenance of two segregated phases in the peptoid 3 film offers insight

into how the presence of the peptoid alkyl chains affects the surfactant layer during compression, thereby improving in vitro surface activity. The alkyl chains assist in a monolayer-to-multilayer transition that thickens the more fluid-like phase. During this process, the alkyl chains act as hydrophobic anchors that keep the peptoid and surrounding lipid species tightly associated with the compressed surface layer, maintaining its interfacial presence at low γ (12). These excluded structures reduce the compressibility of both the fluid phase and the entire film during compression, permitting a rapid reduction to low γ. Upon expansion, these excluded structures are rapidly reincorporated to the interfacial layer to facilitate respreading, reducing γ_{max}. These seemingly antagonistic properties were echoed in the PBS loops, where peptoid 3 improved dynamic cycling properties, resulting in a film that reached low γ with less compression and also had a lower γ_{max}.

Therefore, although all of the peptoids were able to reproduce many of SP-C's biophysical activities, the presence of alkyl chains most increased the extent of biomimicry. The precise role of the thioester-linked palmitoyl chains in SP-C is not known; however, their strict conservation among all species suggests an important role in SP-C and LS homeostasis. SP-C, even in the absence of palmitoylation, has been shown to promote the transfer of material from the a/l interface to the surface-associated bilayer, forming a surfactant reservoir that is reincorporated upon expansion or inhalation (34). However, the palmitoyl chains are required for the formation of multilayered structures upon compression, and avoid irreversible collapse of the fluid-like phase by forming a multilayered, surfactant reservoir (26). Because the palmitoyl chains of SP-C are well-suited for insertion into and interaction with the membrane structures of LS films at high Π, it is likely that the alkyl chains are able to link excluded surfactant material to the a/l surface, forming multilayered surfactant structures (40–43). The presence of the palmitoyl chains would increase the retention and respreading of excluded material during respiration, reducing film compressibility and lowering the γ_{max} during dynamic cycling.

Although some of the biophysical techniques (i.e., PBS absorption and LWSB compression) employed in this study showed little to modest differences upon N-terminal alkylation, other characterization techniques (i.e., dynamic PBS cycling and AFM) revealed greater changes in dynamic surface properties and film morphologies. Therefore, whereas the findings obtained by one technique might suggest only a slight improvement in biophysical activity upon acylation; the results from all of the techniques in combination reveal the full significance of the SP-C-like palmitoylation. This constructed representation supports not only each individual finding but also the broader hypothesis that a palmitoyl-like addition results in the formation of multilayered surfactant structures that remain associated with the a/l surface and significantly improve biomimicry over the nonacylated mimic. This effect is also consistent with previous experimental work that compared acylated and nonacylated SP-C peptides (41).

Taken together, our results show that peptoid-based mimics of SP-C are able to exhibit biophysical activities similar to those of SP-C when combined in a lipid film, and that the extent of the biomimicry is improved by the addition of at least one alkyl chain moiety to the N-terminus. These novel (to our knowledge) species replicate SP-C's key molecular and structural motifs, but their side-chain chemistry and unique backbone structure reduce many of the difficulties associated with handling native SP-C. With their improved stability, favorable production potential, and reduced risk of pathogenic contamination, peptoid-based surfactant replacement therapies have the potential to improve the treatment of infant respiratory distress syndrome as well as other, more prevalent respiratory-related disorders, particularly when greater quantities of surface-active material are warranted, such as in the case of acute respiratory distress syndrome.

SUPPORTING MATERIAL

Additional text, five figures, two tables, and references are available at http://www.biophysj.org/biophysj/supplemental/S0006-3495(11)00650-3.

The authors thank Dr. Jesús Pérez-Gil for the gift of porcine SP-C, and Dr. Mark Johnson and Dr. Ronald Zuckermann for their assistance. J.B.S. also thanks Dr. Adam C. Simonsen for his assistance with the work. The authors acknowledge the Keck Biophysics Instrumentation Facility at Northwestern University for use of the CD instrument.

This work was supported by the National Heart Blood and Lung Institute, National Institutes of Health (No. 2 R01 HL67984), and the National Science Foundation (No. BES-0101195 and Collaborative Research in Chemistry No. CHE-0404704). N.J.B. received support from Northwestern University's NIH Biotechnology predoctoral training program. J.B.S. received project support from the Lundbeck Foundation and a grant from the Danish National Research Foundation, which supports the MEMPHYS-Center for Biomembrane Physics.

REFERENCES

1. Veldhuizen, R., K. Nag, …, F. Possmayer. 1998. The role of lipids in pulmonary surfactant. *Biochim. Biophys. Acta.* 1408:90–108.
2. Almlén, A., G. Stichtenoth, …, T. Curstedt. 2008. Surfactant proteins B and C are both necessary for alveolar stability at end expiration in premature rabbits with respiratory distress syndrome. *J. Appl. Physiol.* 104:1101–1108.
3. Gómez-Gil, L., D. Schürch, …, J. Pérez-Gil. 2009. Pulmonary surfactant protein SP-C counteracts the deleterious effects of cholesterol on the activity of surfactant films under physiologically relevant compression-expansion dynamics. *Biophys. J.* 97:2736–2745.
4. Johansson, J., T. Szyperski, …, K. Wüthrich. 1994. The NMR structure of the pulmonary surfactant-associated polypeptide SP-C in an apolar solvent contains a valyl-rich α-helix. *Biochemistry.* 33:6015–6023.
5. Vandenbussche, G., A. Clercx, …, J. M. Ruysschaert. 1992. Structure and orientation of the surfactant-associated protein C in a lipid bilayer. *Eur. J. Biochem.* 203:201–209.
6. Gonzalez-Horta, A., D. Andreu, …, J. Perez-Gil. 2008. Effects of palmitoylation on dynamics and phospholipid-bilayer-perturbing

properties of the N-terminal segment of pulmonary surfactant protein SP-C as shown by 2H-NMR. *Biophys. J.* 95:2308–2317.

7. Weaver, T. E., and J. J. Conkright. 2001. Function of surfactant proteins B and C. *Annu. Rev. Physiol.* 63:555–578.
8. Oosterlaken-Dijksterhuis, M. A., H. P. Haagsman, …, R. A. Demel. 1991. Characterization of lipid insertion into monomolecular layers mediated by lung surfactant proteins SP-B and SP-C. *Biochemistry.* 30:10965–10971.
9. Taneva, S. G., and K. M. W. Keough. 1994. Dynamic surface properties of pulmonary surfactant proteins SP-B and SP-C and their mixtures with dipalmitoylphosphatidylcholine. *Biochemistry.* 33:14660–14670.
10. Takamoto, D. Y., M. M. Lipp, …, J. A. Zasadzinski. 2001. Interaction of lung surfactant proteins with anionic phospholipids. *Biophys. J.* 81:153–169.
11. von Nahmen, A., M. Schenk, …, M. Amrein. 1997. The structure of a model pulmonary surfactant as revealed by scanning force microscopy. *Biophys. J.* 72:463–469.
12. Brown, N. J., J. Johansson, and A. E. Barron. 2008. Biomimicry of surfactant protein C. *Acc. Chem. Res.* 41:1409–1417.
13. Gustafsson, M., J. Thyberg, …, J. Johansson. 1999. Amyloid fibril formation by pulmonary surfactant protein C. *FEBS Lett.* 464:138–142.
14. Wu, C. W., S. L. Seurynck, …, A. E. Barron. 2003. Helical peptoid mimics of lung surfactant protein C. *Chem. Biol.* 10:1057–1063.
15. Brown, N. J., C. W. Wu, …, A. E. Barron. 2008. Effects of hydrophobic helix length and side chain chemistry on biomimicry in peptoid analogues of SP-C. *Biochemistry.* 47:1808–1818.
16. Zuckermann, R. N., J. M. Kerr, …, W. H. Moos. 1992. Efficient method for the preparation of peptoids oligo(n-substituted glycines) by submonomer solid-phase synthesis. *J. Am. Chem. Soc.* 114:10646–10647.
17. Wu, C. W., K. Kirshenbaum, …, A. E. Barron. 2003. Structural and spectroscopic studies of peptoid oligomers with α-chiral aliphatic side chains. *J. Am. Chem. Soc.* 125:13525–13530.
18. Armand, P., K. Kirshenbaum, …, E. K. Bradley. 1998. NMR determination of the major solution conformation of a peptoid pentamer with chiral side chains. *Proc. Natl. Acad. Sci. USA.* 95:4309–4314.
19. Sanborn, T. J., C. W. Wu, …, A. E. Barron. 2002. Extreme stability of helices formed by water-soluble poly-N-substituted glycines (polypeptoids) with α-chiral side chains. *Biopolymers.* 63:12–20.
20. Plasencia, I., K. M. W. Keough, and J. Perez-Gil. 2005. Interaction of the N-terminal segment of pulmonary surfactant protein SP-C with interfacial phospholipid films. *Biochim. Biophys. Acta.* 1713:118–128.
21. Pérez-Gil, J., A. Cruz, and C. Casals. 1993. Solubility of hydrophobic surfactant proteins in organic solvent/water mixtures. Structural studies on SP-B and SP-C in aqueous organic solvents and lipids. *Biochim. Biophys. Acta.* 1168:261–270.
22. Seurynck, S. L., N. J. Brown, …, M. Johnson. 2005. Optical monitoring of bubble size and shape in a pulsating bubble surfactometer. *J. Appl. Physiol.* 99:624–633.
23. Bringezu, F., J. Q. Ding, …, J. A. Zasadzinski. 2001. Changes in model lung surfactant monolayers induced by palmitic acid. *Langmuir.* 17:4641–4648.
24. Abramoff, M. D., P. J. Magelhaes, and S. J. Ram. 2004. Image processing with ImageJ. *Biophoton. Int.* 11:36–42.
25. Dohm, M. T., N. J. Brown, …, A. E. Barron. 2010. Mimicking SP-C palmitoylation on a peptoid-based SP-B analogue markedly improves surface activity. *Biochim. Biophys. Acta.* 1798:1663–1678.
26. Na Nakorn, P., M. C. Meyer, …, H. J. Galla. 2007. Surfactant protein C and lung function: new insights into the role of α-helical length and palmitoylation. *Eur. Biophys. J.* 36:477–489.
27. Wang, Z. D., S. B. Hall, and R. H. Notter. 1996. Roles of different hydrophobic constituents in the adsorption of pulmonary surfactant. *J. Lipid Res.* 37:790–798.
28. Johansson, J., T. Curstedt, and B. Robertson. 2001. Artificial surfactants based on analogues of SP-B and SP-C. *Pediatr. Pathol. Mol. Med.* 20:501–518.
29. Smith, E. C., J. M. Crane, …, S. B. Hall. 2003. Metastability of a supercompressed fluid monolayer. *Biophys. J.* 85:3048–3057.
30. Gopal, A., and K. Y. C. Lee. 2001. Morphology and collapse transitions in binary phospholipid monolayers. *J. Phys. Chem. B.* 105:10348–10354.
31. Nag, K., J. Perez-Gil, …, K. M. Keough. 1996. Fluorescently labeled pulmonary surfactant protein C in spread phospholipid monolayers. *Biophys. J.* 71:246–256.
32. Pérez-Gil, J., K. Nag, …, K. M. Keough. 1992. Pulmonary surfactant protein SP-C causes packing rearrangements of dipalmitoylphosphatidylcholine in spread monolayers. *Biophys. J.* 63:197–204.
33. Amrein, M., A. von Nahmen, and M. Sieber. 1997. A scanning force- and fluorescence light microscopy study of the structure and function of a model pulmonary surfactant. *Eur. Biophys. J.* 26:349–357.
34. Ding, J. Q., D. Y. Takamoto, …, J. A. Zasadzinski. 2001. Effects of lung surfactant proteins, SP-B and SP-C, and palmitic acid on monolayer stability. *Biophys. J.* 80:2262–2272.
35. Crane, J. M., and S. B. Hall. 2001. Rapid compression transforms interfacial monolayers of pulmonary surfactant. *Biophys. J.* 80:1863–1872.
36. Walters, R. W., R. R. Jenq, and S. B. Hall. 2000. Distinct steps in the adsorption of pulmonary surfactant to an air-liquid interface. *Biophys. J.* 78:257–266.
37. Krüger, P., J. E. Baatz, …, M. Lösche. 2002. Effect of hydrophobic surfactant protein SP-C on binary phospholipid monolayers. Molecular machinery at the air/water interface. *Biophys. Chem.* 99:209–228.
38. Kramer, A., A. Wintergalen, …, R. Guckenberger. 2000. Distribution of the surfactant-associated protein C within a lung surfactant model film investigated by near-field optical microscopy. *Biophys. J.* 78:458–465.
39. Perez-Gil, J. 2008. Structure of pulmonary surfactant membranes and films: the role of proteins and lipid-protein interactions. *Biochim. Biophys. Acta.* 1778:1676–1695.
40. Bi, X. H., C. R. Flach, …, R. Mendelsohn. 2002. Secondary structure and lipid interactions of the N-terminal segment of pulmonary surfactant SP-C in Langmuir films: IR reflection-absorption spectroscopy and surface pressure studies. *Biochemistry.* 41:8385–8395.
41. Gustafsson, M., M. Palmblad, …, S. Schurch. 2000. Palmitoylation of a pulmonary surfactant protein C analogue affects the surface associated lipid reservoir and film stability. *Biochim. Biophys. Acta.* 1466:169–178.
42. Plasencia, I., F. Baumgart, …, J. Perez-Gil. 2008. Effect of acylation on the interaction of the N-Terminal segment of pulmonary surfactant protein SP-C with phospholipid membranes. *Biochim. Biophys. Acta.* 1778:1274–1282.
43. ten Brinke, A., L. M. G. van Golde, and J. J. Batenburg. 2002. Palmitoylation and processing of the lipopeptide surfactant protein C. *Biochim. Biophys. Acta.* 1583:253–265.